

## Measurement of Chiral-Dependent Magnetic Anisotropy in Carbon Nanotubes

Omar N. Torrens,<sup>†</sup> Daniel E. Milkie,<sup>†</sup> Han Y. Ban,<sup>†</sup> Ming Zheng,<sup>‡</sup> G. Bibiana Onoa,<sup>‡</sup>  
Timothy D. Gierke,<sup>‡</sup> and James M. Kikkawa<sup>\*,†</sup>

Department of Physics and Astronomy, University of Pennsylvania, Philadelphia, Pennsylvania 19104, and  
DuPont Central Research and Development, Experimental Station, Wilmington, Delaware 19880

Received September 18, 2006; E-mail: kikkawa@physics.upenn.edu

Orbital magnetic susceptibility anisotropy  $\Delta\chi$  has played an important role as a probe of electron delocalization in aromatic systems.<sup>1</sup> Single-walled carbon nanotubes (SWNTs) are  $\pi$ -conjugated molecules structurally between fullerenes and planar graphene,<sup>2</sup> heavily investigated for their use in nanotechnology and advanced composites. Carrier delocalization is important for nearly all SWNT properties, and yet  $\Delta\chi$  is not well understood in these systems. Here, our experimental measurements determine  $\Delta\chi$  for several SWNT species and combine with theory to forecast  $\Delta\chi$  for all species of semiconducting SWNTs.

The earliest studies of SWNT magnetism utilized a  $\pi$  band framework, predicting that  $\Delta\chi$  would depend on diameter and whether a SWNT was semiconducting or metallic but on no other structural details.<sup>3</sup> Very recent ab initio calculations, however, show departure from those predictions, and indicate  $\Delta\chi$  varies substantially among semiconducting species of nearly equal diameters.<sup>4</sup> Yet, issues related to sample composition have hampered experimental verification of either prediction, as isolation of SWNTs from other chiral species and growth catalysts has proven difficult. Ferromagnetism associated with the latter was found to strongly influence magnetic anisotropy measurements,<sup>5</sup> so that even the basic prediction that SWNTs are intrinsically well described by a linear orbital magnetic susceptibility<sup>3</sup> has never been carefully tested.

In this work, the combination of a chiral-selective optical spectroscopy and a magnetically pure sample overcomes these obstacles. The essential procedure is to obtain  $\Delta\chi$  from the magnetic alignment of SWNTs suspended in H<sub>2</sub>O using DNA.<sup>6</sup> We use polarization-resolved resonant photoluminescence (PL) to sensitively measure the nematic order parameter<sup>5,7</sup>  $S$  quantifying SWNT alignment. Even in state-of-the-art samples, polydispersity leads to overlapping optical resonances that can complicate single-wavelength absorptive<sup>5</sup> or emissive<sup>8</sup> alignment studies. Here, the associated systematic errors are avoided by choosing nondegenerate excitation and detection energies that resonantly target single species<sup>9</sup> and discriminate against carbonaceous impurities. The resulting  $S(B)$  shows no trace of catalyst-assisted alignment and is fit to obtain  $\Delta\chi$  directly without assumptions regarding changes in bandstructure or the radiative efficiencies of Aharonov–Bohm emission pairs.<sup>8</sup>

The SWNT population of our sample permits accurate alignment and  $\Delta\chi$  studies for (6,4), (8,3), (6,5), and (7,5) chiralities, where the wrapping vector  $(n,m)$  describes the SWNT atomic structure.<sup>2</sup> Figure 1 shows the measured field dependence of  $S$  and  $P_4$ , the second and fourth moments of the SWNT orientational distribution function  $f$ , respectively.<sup>7</sup>  $S \equiv (1/2)(3 \cos^2 \phi - 1)$  is the so-called nematic order parameter (brackets indicate ensemble averaging over  $f$  and  $\phi$  is the angle between the field and nanotube axes), and since both  $S$  and  $P_4$  equal zero for an isotropic ensemble and unity for

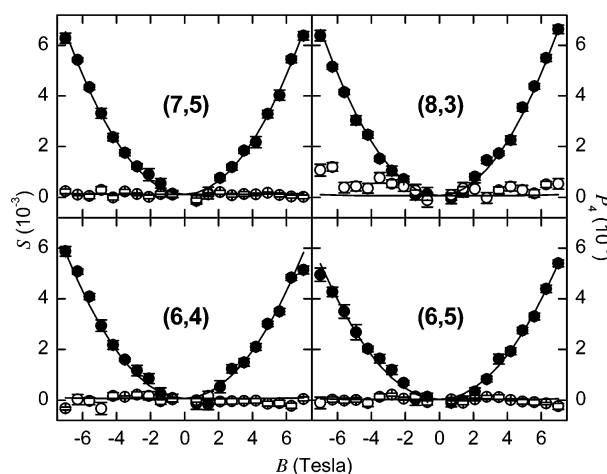


**Figure 1.** Nanotube alignment measured by polarized PL. Shown are  $S$  (filled circles) and  $P_4$  (open circles) for (8,3), (6,4), (7,5), and (6,5) semiconducting species. Resonant excitation and collection wavelengths are chosen to provide a background-free measurement of the indicated chirality. Solid lines are fits described in the text.

complete alignment, the data indicate a rather small degree of alignment. Notably,  $S(B)$  demonstrates the intrinsic linear-orbital behavior that has been anticipated for SWNTs,<sup>3</sup> showing no contribution from catalyst moment anisotropy.<sup>5</sup> Accordingly, several field sweeps are averaged to provide an accuracy of better than  $5 \times 10^{-4}$ . The analysis used to present these data takes into account the intrinsic optical anisotropies,<sup>7</sup> detector quantum efficiencies, and any field-dependent PL efficiencies. Fits of  $S(B)$  for each  $(n,m)$  use a sample length distribution (assumed independent of chirality) measured by atomic force microscopy (AFM), and apart from offsets of  $\sim 10^{-4}$ , involve only a single free parameter,  $\Delta\chi$ . These values of  $\Delta\chi$  are then used to predict  $P_4(B)$ , which shows good agreement with our data indicating self-consistency of the underlying Boltzmann model,  $f \propto \exp\{-U/kT\}$  (where  $U = -(1/2)\Delta\chi B^2 \cos^2 \phi$  is the magnetic anisotropy energy). The regular wrapping and known values of  $\mathbf{G}$  and  $\mathbf{T}$  nucleobase magnetic susceptibility tensors<sup>10</sup> allow us to subtract the DNA contribution ( $\Delta\chi_{\text{DNA}} = (0.89 \pm 0.30) \times 10^{-6}$  emu per mole SWNT carbon), which is nevertheless small ( $\sim 5\%$ ).

Figure 2A shows the resulting  $\Delta\chi_{(n,m)}$  divided by diameter  $D$ , giving the first clear experimental evidence for a departure from large- $D$  calculations which gave a constant  $\Delta\chi/D$  for all semiconducting species.<sup>3</sup> More recent ab initio calculations<sup>4</sup> have, however, predicted differences which are more easily discussed in terms of chiral index,  $\nu \equiv (n - m) \bmod 3 = \{0, \pm 1\}$ , and chiral angle,  $\theta = \tan^{-1}[\sqrt{3}m/(2n + m)]$ . In particular, these calculations show chiral-dependent deviations of opposite sign depending on whether  $\nu = +1$  or  $\nu = -1$ . These predictions were made only for “zigzag” nanotubes, whose chiral angle ( $\theta = 0$ ) differs from those studied

<sup>†</sup> University of Pennsylvania.

<sup>‡</sup> DuPont Central Research and Development, Experimental Station.

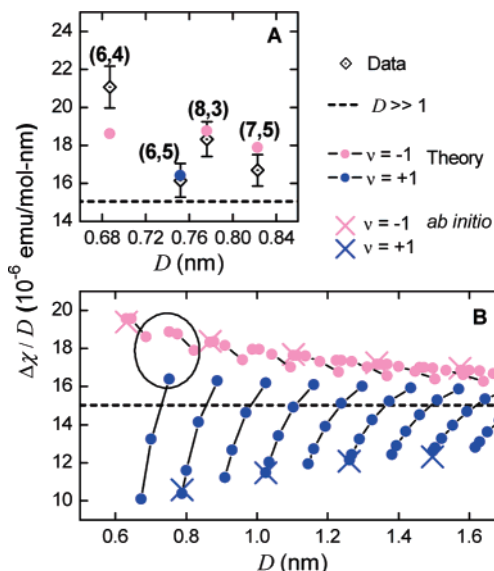


**Figure 2.** Experimental and theoretical magnetic anisotropies. (A) Measured  $\Delta\chi/D$  (open diamonds) and theoretical values (colored dots); (B) ab initio calculations<sup>4</sup> (crosses) and theoretical generalization for  $\Delta\chi/D$  described in the text, with SWNTs in the same  $2n + m$  family connected by lines. The circle indicates the range of chiralities from A. In A and B, dashed line indicates the large-diameter limit and purple (blue) dots indicate theory for  $\nu = \pm 1$ .

here. Nonetheless, structural symmetry arguments significantly restrict how one may extend these predictions to any semiconductor chirality,<sup>11</sup> and our measurements of  $\Delta\chi$  give important evidence for asymmetry between  $\nu = \pm 1$  nanotubes.

For any scalar observable  $Q$  that does not distinguish between the ends of a SWNT and is insensitive to SWNT right- or left-handedness,  $Q = \sum_{n=0}^{\infty} \gamma_n \cos 6n\theta + \delta_n \cos(6n\theta + 3\theta)$ , where the coefficients  $\gamma_n$  and  $\delta_n$  depend on  $D$  and whether  $\nu = \pm 1$  (semiconducting) or  $\nu = 0$  (metallic).<sup>11</sup> In the semiconducting or metallic case, if  $Q$  scales as  $D^p$  in the large- $D$  limit one can expand  $Q/D^p$  in powers of  $(1/D)$  as

$$\frac{Q}{D^p} = a_0 + \frac{1}{D}(b_0 + b_1\nu \cos 3\theta + b_2 \cos 6\theta + \dots) + \frac{1}{D^2}(c_0 + c_1\nu \cos 3\theta + \dots) + \dots$$

where the set of coefficients  $\{a_0, b_i, c_j, \dots\}$  is independent of  $D$ . Mathematical expressions including  $\cos 3\theta$  terms have often been used to empirically fit the chirality dependence of the effects of trigonal warping and curvature on SWNT subband energies<sup>11,12</sup> and their ratios<sup>9</sup> as a function of  $D$ . Other quantities that “fan away” from their large diameter scaling limit as a function of  $D$  and chirality have been modeled in a similar fashion, including electron effective mass,<sup>13</sup> Raman radial breathing mode frequency, Raman G-band frequency, and their intensities.<sup>13,14</sup>

To compare with our findings, the minimal generalization of the ab initio calculations would expand  $\Delta\chi/D$  using the first three terms in the  $Q/D^p$  expansion. The first coefficient  $a_0$  is the large diameter limit, for which both ab initio and large-diameter theories are in accord. The second and third terms,  $(b_0 + b_1\nu \cos 3\theta)/D$ , then model the ab initio calculations, which were made for  $\nu = \pm 1$ ,  $\theta = 0$ . Our data reveal the minimal model necessary, however, and imply that the fourth term  $(b_2 \cos 6\theta)/D$ , is additionally necessary to break the symmetry among  $\nu = \pm 1$  states about the large diameter limit. Such asymmetry is a hallmark of other SWNT physical properties.<sup>9,13–15</sup> Including the fourth term, we note that  $a_0 = 15.0 \times$

$10^{-6}$  emu/(mol·nm) remains set by the large-diameter limit, while (in units of  $10^{-6}$  emu/mol)  $b_1 = -3.25$  and  $(b_0 + b_2) = -0.40$  are set by the zigzag calculations. The values of  $\Delta\chi$  measured here are therefore used to set only a single coefficient,  $b_2 = -0.99 \pm 0.19$ , with the resulting extrapolated theory shown in Figure 2A for the chiralities studied here, and in Figure 2B for all semiconducting species in a larger  $D$  range. Notably, qualitative trends in the data are reproduced in the theory, and one even finds reasonable quantitative agreement (Figure 2A).

In summary, we present species-resolved polarized PL measurements of SWNT magnetic anisotropies. DNA-SWNTs show no sign of impurity moment anisotropy, permitting intrinsic SWNT properties to dominate the measurement. Our results show differences in magnetism among SWNT chiralities that, in conjunction with theory, help to construct a fan-out diagram for predicting magnetic anisotropies of arbitrary semiconducting SWNTs. In the future, combining these experimental and analytical techniques with resonant Raman or Rayleigh scattering could target metallic species.

**Acknowledgment.** We thank Eugene J. Mele for helpful discussions and Paul Frail for his assistance in obtaining SWNT length distributions. We acknowledge support from NSF MRSEC DMR-0520020 and NSF CAREER DMR-0094156 and partial support from DARPA through ONR N00015-01-1-0831.

**Supporting Information Available:** Experimental and analytical methods, optical and magnetic SWNT characterization data, calculation of DNA magnetic anisotropy, error estimation. This material is available free of charge via the Internet at <http://pubs.acs.org>.

## References

- (a) Schmalz, T. G.; Norris, C. L.; Flygare, W. H. *J. Am. Chem. Soc.* **1973**, *95*, 7961–7967. (b) Schmalz, T. G.; Gierke, T. D.; Beak, P.; Flygare, W. H. *Tetrahedron Lett.* **1974**, *33*, 2885–2888.
- Saito, R.; Dresselhaus, G.; Dresselhaus, M. S. *Physical Properties of Carbon Nanotubes*; Imperial College Press: London, 1998.
- (a) Lu, J. P. *Phys. Rev. Lett.* **1995**, *74*, 1123–1126. (b) Ajiki, H.; Ando, T. *J. Phys. Soc. Jpn.* **1995**, *64*, 4382–4391.
- Marques, M. A. L.; d’Avezac, M.; Mauri, F. *Phys. Rev. B: Condens. Matter* **2006**, *73*, 125433.
- Islam, M. F.; Milkie, D. E.; Torrens, O. N.; Yodh, A. G.; Kikkawa, J. M. *Phys. Rev. B: Condens. Matter* **2005**, *71*, 201401.
- (a) Zheng, M.; Jagota, A.; Strano, M. S.; Santos, A. P.; Barone, P.; Chou, S. G.; Diner, B. A.; Dresselhaus, M. S.; McLean, R. S.; Onoa, G. B.; Samsonidze, G. G.; Semke, E. D.; Usrey, M.; Walls, D. J. *Science* **2003**, *302*, 1545–1548. (b) Huang, X. Y.; McLean, R. S.; Zheng, M. *Anal. Chem.* **2005**, *77*, 6225–6228.
- Michl, J.; Thulstrup, E. W. *Spectroscopy with Polarized Light*; VCH Publishers, Inc.: New York, 1986.
- Zaric, S.; Ostojic, G. N.; Kono, J.; Shaver, J.; Moore, V. C.; Hauge, R. H.; Smalley, R. E.; Wei, X. *Nano Lett.* **2004**, *4*, 2219–2221.
- Bachilo, S. M.; Strano, M. S.; Kittrell, C.; Hauge, R. H.; Smalley, R. E.; Weisman, R. B. *Science* **2002**, *298*, 2361–2366.
- (a) Bryce, D. L.; Boisbouvier, J.; Bax, A. *J. Am. Chem. Soc.* **2004**, *126*, 10820–10821. (b) Bryce, D. L. Personal communication.
- Ye, F.; Wang, B. S.; Su, Z. B. *Phys. Rev. B: Condens. Matter* **2004**, *70*, 153406.
- (a) Yorikawa, H.; Muramatsu, S. *Phys. Rev. B: Condens. Matter* **1994**, *50*, 12203–12206. (b) Reich, S.; Thomsen, C. *Phys. Rev. B: Condens. Matter* **2000**, *62*, 4273–4276. (c) Strano, M. S.; Doorn, S. K.; Haroz, E. H.; Kittrell, C.; Hauge, R. H.; Smalley, R. E. *Nano Lett.* **2003**, *3*, 1091–1096. (d) Kane, C. L.; Mele, E. J. *Phys. Rev. Lett.* **1997**, *78*, 1932–1935. (e) Maultzsch, J.; Telg, H.; Reich, S.; Thomsen, C. *Phys. Rev. B: Condens. Matter* **2005**, *72*, 205438.
- Jorio, A.; Fantini, C.; Pimenta, M. A.; Capaz, R. B.; Samsonidze, G. G.; Dresselhaus, G.; Dresselhaus, M. S.; Jiang, J.; Kobayashi, N.; Gruneis, A.; Saito, R. *Phys. Rev. B: Condens. Matter* **2005**, *71*, 075401.
- (a) Popov, V. N.; Lambin, P. *Phys. Rev. B: Condens. Matter* **2006**, *73*, 085407. (b) Popov, V. N.; Lambin, P. *Phys. Rev. B: Condens. Matter* **2006**, *73*, 165425.
- Oyama, Y.; Saito, R.; Sato, K.; Jiang, J.; Samsonidze, G. G.; Gruneis, A.; Miyauchi, Y.; Maruyama, S.; Jorio, A.; Dresselhaus, G.; Dresselhaus, M. S. *Carbon* **2006**, *44*, 873–879.

JA066719+